Int. J. Electrochem. Sci., 7 **(2012)** 5297 - 5313

International Journal of
ELECTROCHEMICAL
SCIENCE
www.electrochemsci.org

Synthesis, Characterization, Electrocatalytic and Catalytic Activity of Thermally Generated Polymer-Stabilized Metal Nanoparticles

Egwu E. Kalu[1,*], *Mimi Daniel*[1] *and Michael R. Bockstaller*[2]

[1] Department of Chemical & Biomedical Engineering, FAMU-FSU College of Engineering, Tallahassee, FL 32310, USA
[2] Department of Materials Science and Engineering, Carnegie Mellon University Pittsburgh, PA, USA
[*]E-mail: ekalu@eng.fsu.edu

Received: 3 April 2012 / *Accepted:* 14 May 2012 / *Published:* 1 June 2012

Polymer-stabilized metal nanoparticles were prepared without chemical reducing agent by facile thermolysis of metal-polymer complex at a relatively low temperature and evidence of formation of zero-valent metal nanoparticles elucidated through the use of TEM, XRD and electrochemical techniques. The polymer-stabilized Pd nanoparticles were found catalytically active for oxygen electrocatalysis, electroless deposition of metals, and the hydrolysis of ammonia-borane for hydrogen generation. The catalytically active metal nanoparticles were characterized by UV-vis spectroscopy (UV-vis), transmission electron microscopy (TEM), x-ray diffraction spectroscopy (XRD), optical microscopy (OM) and electrochemical techniques. The electrocatalysis of oxygen reduction in 0.5 M H_2SO_4 and hydrogen peroxide oxidation in 0.1 M phosphate buffer solution (pH 7) were used as illustrative examples of the electrocatalytic activity of polyvinyl butyral (PVB)-stabilized Pd nanoparticles prepared by the reported method.

Keywords: Electrocatalysis; polymer-stabilized; thermolysis; nanoparticles; nanocomposite; hydrolysis; hydrogen generation; catalysis

1. INTRODUCTION

Physical or chemical methods [1 - 5] are often used to prepare metal nanoparticles on chemically inert supports with large surface areas for heterogeneous catalysis on inorganic oxides [6 – 9] and carbon materials [1, 10]. The chemical route for nanoparticle preparation involves the reduction of one or more metal ions to their zero-valent atoms. The objective in catalyst synthesis is to produce

small, well dispersed, discrete and uniformly sized nanoparticles that are uniformly distributed on the carrier. The particle size not only affects the catalyst activity but can also determine the catalyst selectivity.

The incipient wetness impregnation method is the most widely used method in the preparation of catalysts [11-12]. In this method, the purified carrier is impregnated with a solution of the metal precursor, then dried, calcined and/or reduced to obtain nanoparticles dispersed on the support. The approach may involve use of temperatures up to 300 ^{o}C or more to decompose the precursor salt. In many cases, the uniformity of nanoparticle size and their distributions are well controlled. However, research efforts are still being expended to develop better synthetic techniques to address the shortcomings of the method. Other synthesis routes studied include the deposition precipitation method [13, 14], metal-ion adsorption [15] and the physical method of chemical vapor deposition [16].

Intense investigation and research in nanoparticle synthesis in the past decade can be traced to the realization that exploitation of nanoparticles for device fabrication requires the formation of morphologically controlled or highly ordered arrays of nanoparticles [17 -19]. This is especially true for the case of the development of well dispersed Pt nanoparticles on carbon for fuel cell applications. Unfortunately, Pt-based catalysts are expensive and thus minimization of the amount of Pt usage with optimal cell performance drives the current research effort in the area. The major challenge is to be able to control the structural arrangements of the nanoparticles in order to reach the goal of minimal (Pt) usage with maximum catalyst performance. Polymer or ligand stabilized metal nanoparticles assembly is an attempt to utilize polymer or its ligand properties for the controlled assembly of nanoparticles [20 – 23]. Controlled assembly of metal nanoparticles with the aid of polymer mediation may lead to the minimization of amount of expensive transition metal (Pt, Au) required for catalysis. Several publications on the use of polymer mediation in the synthesis of mono-metallic or bimetallic catalysts have appeared in the literature [1, 6, 9]. The general approach reported in the literature for the formation of metal nanoparticles involves direct reduction of metal salt by the solvent (e.g. glycol) at high temperature or by the use of a chemical reducing agent (e.g. $NaBH_4$) all carried out in the presence of a polymer stabilizer. Following the formation of nanoparticles in the polymer-stabilized media, some authors embark on centrifugation for nanoparticle recovery while others describe the thermolysis of the polymer-metal-reducing agent mixture to create an active catalyst surface.

Crooks and his group [6, 9, 23] and several others utilized hydroxyl- and amine-terminated dendrimers (G6-OH and G6-NH_2) in the synthesis of metal dendrimer-encapsulated catalysts including electrocatalysts for oxygen reduction. A long and complex synthetic method that may take several hours or days for the dissolution of metal precursor is used in the dendrimer approach. Use is made of a chemical reducing agent, $NaBH_4$ for the formation of the nanoparticles in the dendrimer polymer matrix. That is, a chemical reduction is first used for the formation of the metal nanoparticles that are subsequently stabilized by the polymer. In order to expose the encapsulated metal nanoparticles for electrocatalysis, the authors embarked on further thermolysis of the polymer-metal composite. A simple and direct preparation method by which the above described is shortened will be useful both from applications point of view and fundamental studies. Such shortened methods may include the use of UV and γ-irradiation [24, 25] and controlled thermal treatment [26].

Herein, we report a facile and thermally induced method to generate dispersed active metal nanoparticles stabilized in a polymer matrix with or without solid supports. No additional chemical reducing agent is used except the stabilizing polymer and the solvent used for the polymer. It is an additional tool that can be used to prepare certain active metal nanoparticles catalysts at relatively low temperatures. The advantage of the approach is that (i) it is simple and does not require sophisticated equipment (ii) can be used for patterning on any substrate (iii) different polymer samples can be used (iv) does not require aggressive reducing agents. The method is illustrated using Pd as a sample metal and Poly-Vinyl Butyral (PVB) as the polymer sample. Transmission electron microscopy (TEM), UV-vis spectrophotometer and electrochemical techniques were used to characterize the nanocomposites. The electrocatalytic activity of polymer-stabilized Pd nanoparticles for oxygen reduction in 0.5 M H_2SO_4 and its use for the oxidation of hydrogen peroxide in 0.1 M phosphate buffer solution at pH 7 are illustrated by cyclic voltammetry. We also illustrate the use of the polymer-stabilized Pd nanoparticles for catalysis of electroless Ni metallization of Al_2O_3 particles and its use for the hydrolysis of ammonia-borane (both) for hydrogen generation.

2. EXPERIMENTAL SECTION

2.1 Preparation of Polymer-Stabilized Nanoparticles

The preparation of the polymer-stabilized catalyst solution used a method described in detail elsewhere [27 – 29]. The polymer-stabilized palladium catalyst solution was prepared by dissolving 0.2 g analytical reagent grade palladium acetate $[CH_3CO_2)_2Pd]$ (47.05 % Pd) from Aldrich-Sigma Co, in 2.0 ml NH_4OH. The palladium mixture was then added with stirring to a 44 g methanol-poly (vinyl) butyral (Solutia Inc.'s Butvar B-98) mixture formed by dissolving 22 g PVB in 140 ml methanol. After a thorough mixing, the as-prepared catalyst solution can be preserved for years without loss in its activity.

2.2 Preparation of Supported Catalyst

In order to prepare supported catalyst, a weighed amount (5 g) of graphite powder (-200 mesh) was thoroughly mixed with an equal amount (by weight) of the polymer-catalyst solution. The catalyzed particles were dried and thermally activated in an oven at different temperatures for 2 hours or longer. This is equivalent to a loading of 1.842 μg Pd/g catalyst. To prepare catalyst ink, 0.30 g of metal-catalyzed graphite particles and 0.60 g Nafion were mixed together with small DI water and sonicated for 10 minutes. For the present work, we used 3 mm (diameter) glassy carbon as the substrate for the graphite-supported catalysts. The catalyst-ink (2 μL) was deposited on the surface of the working electrode and allowed to dry at room temperature for 60 minutes. An uncatalyzed graphite-ink was also prepared.

2.2 Characterization of Polymer-Stabilized Nanoparticles

2.2.1. UV-vis, TEM and XRD Characterizations:

The polymer-metal solutions were dropped and spread on microscopic glass slides with micro-pipette. The glass slides with polymer-metal thin films were first dried in air and then annealed in a vacuum oven at given temperature and time. For the present study, the effect of activation time at room temperature, 100 ^{o}C and 200 ^{o}C was investigated. The glass-slide coated polymer-metal thin film was used for UV-vis spectroscopic analysis. UV-vis measurements were carried out with Cary 300 UV-vis-NIR spectrophotometer (Varian Instruments) over the range 200 – 800 nm.

Transmission Electron Microscopic (TEM) images were obtained using a JEOL JEM-2000 EX II operating at 160 kV. The TEM samples were prepared by placing a drop of the polymer-metal solution on a 400 mesh carbon-coated copper grid. The solution was dried at room temperature and then annealed at the required temperature and time.

For the supported catalyst, one gram of carbon nanotubes (CNT) was mixed with one gram of polymer-metal complex solution to make an ink. After a thorough mixing, the CNT catalyzed sample was activated at 275 ^{o}C between 2 to 24 hours. X-ray Diffraction (XRD) data of the activated catalyst on CNT support was obtained using Philips X'Pert X-ray Diffractometer with Cu Kα radiation (λ = 0.1544 nm). The XRD patterns were recorded between 10^{o} to 90^{o} at a step time of 0.25 s per 0.02^{o}.

2.2.2. Electrochemical Characterization

For electrochemical characterization, a drop of the polymer-metal solution was placed on a polished graphite electrode (3 mm diameter), allowed to dry at room temperature and then annealed for 2 hours at 300^{o}C. After cooling down to room temperature, the nanoparticle-catalyzed electrodes were cycled in 0.5 M H_2SO_4 until the CV showed reproducible voltammograms. After each experimental run, the electrode was washed with deionized water. Cyclic voltammetry of 0.1 M or 6 mM ferricyanide solution was used to evaluate the electrocatalytic activity of the nanoparticles.

For electrochemical characterization of the carbon supported catalyst, 0.10 g of the activated sample was mixed with 0.20 g of Perfluorosulfonic acid (Nafion) from Alfa Aesar. A drop of the resulting catalyst-ink (2 μL) was deposited on the surface of the working electrode and allowed to air dry at room temperature. An uncatalyzed graphite-ink was also prepared. The electrode was cycled in 0.5 M H_2SO_4 until minimum changes in the voltammograms were observed.

2.2.3. Electrochemical Measurements

A Solatron potentiostat interfaced to a PC system equipped with Corrware software (Scribner Associates Inc, NC) was used for the electrochemical studies of the polymer-stabilized metal catalysts. The investigations of oxygen reduction in acid medium and the oxidation of hydrogen peroxide in a phosphate buffer by Pd-based alloy electrocatalysts synthesized by the described routes were carried

out. Cyclic voltammetric techniques were conducted at 5 – 50 mV/s scan rate in both stirred and unstirred solutions. Solution was purged with argon (or nitrogen) or oxygen as the case demands.

2.2.4. Electroless Characterization

The polymer-stabilized metal nanoparticles can be used directly as a catalyst for chemical reactions of interest or as electroless deposition seed catalyst for the deposit of other metal or metal alloys for catalysis of reactions of interest. Electroless deposition of nickel for hydrogen generation from $NaBH_4$ and direct use of polymer-stabilized Pd nanoclusters for ammonia borane hydrolysis for hydrogen generation are used in the present work to characterize the catalyst.

Polymer-Pd catalyst ink was applied on Al_2O_3 particles substrate as seed for electroless Ni. The catalyzed Al_2O_3 sample was air dried for 24 hours and then activated in a furnace (Marshall Split Furnace) for 2 hours in a porcelain boat at a temperature of 250 ^oC. The activation process ensures that Pd^{2+} is reduced to Pd^0. The reduced Pd^0 is the nucleation point for building the nanoparticles of nickel on the surface of Al_2O_3 substrate where palladium acts as the initiator for nickel plating. The activated Al_2O_3 sample was plated in a Ni electroless bath for 2 minutes. The pH of the electroless solution was kept between pH 10 - 11 by a drop-wise addition of ammonium hydroxide. The electroless plating solution contained 7 g/L $NiSO_4.6H_2O$, 10 g/L sodium hypophosphite, 10 g/L sodium-potassium tartrate and 15 g/L D-gluconic acid. A magnetic stirrer was used to stir the Al_2O_3 particles through out the plating duration.

Hydrogen generation performance tests were conducted in a conical flask with 0.1 g of electrolessly plated Al_2O_3 particles placed in a 30 ml of 0.1M $NaBH_4$ solution that was stabilized with NaOH. No stirring was employed in the reaction flask. The water bath temperature was maintained at 34 °C. Volumes of evolved hydrogen gas were measured by recording the displacement of water level in a pipette at atmospheric pressure of 760 mm Hg. Cumulative volumes of hydrogen gas evolved with respect to time were noted for each run.

2.2.5. Ammonia Borane (AB) Hydrolysis Characterization

Polymer stabilized Pd nanoclusters on TiO_2 substrate was prepared as described in [30]. The catalytic activity of activated TiO_2/Pd catalyst in the hydrolysis of AB was determined by measuring the rate of hydrogen generation. In all the experiments, the reaction flask containing the aqueous AB solution was placed in a thermostat that was equipped with a water circulating system to minimize the temperature rise resulting from the highly exothermic hydrolysis reaction. AB solution was preheated and held at the desired temperature, and then certain amount of TiO_2/Pd catalyst was added into the reaction flask. The reaction was started by closing the flask and the volume of hydrogen gas evolved was measured by recording the displacement of water level from the graduated burette as the reaction progressed. No stirring was carried out during the hydrolysis reaction.

3. RESULTS AND DISCUSSION

The polymer type used for the nanoparticle stabilization, its ligand and active functional groups affect the resulting metal nanoparticle size, shape or surface reactivity. These functional groups in the polymer that act as the anchor for the metal nanoparticles are often susceptible to thermal degradation. Thus, as the polymer-alcoholic solution-metal ion mixture is subjected to thermal or reducing treatment, changes occur in the polymer backbone structure including the degradation of the functional groups and a subsequent reduction of the metal ion to its zero-valent state. The reducing agents for the metal ions include the interstitial solvent and the by-products resulting from the decomposition of the polymer functional groups. The structural changes in the polymer backbone are often manifested in the form of observable color variation in the resulting polymer thin film and evolved gases. The multifunctional nature of PVB presents it with several possible mechanisms for degradation. Thus, several products can result from either the degradation of the butyral group or the side chains. For the butyral group, Bakht [31] proposed a cyclic-elimination mechanism that involves the release of aldehyde (metal reducing agent) and unsaturated end-groups at temperatures between 250^{o}C - 300^{o}C.

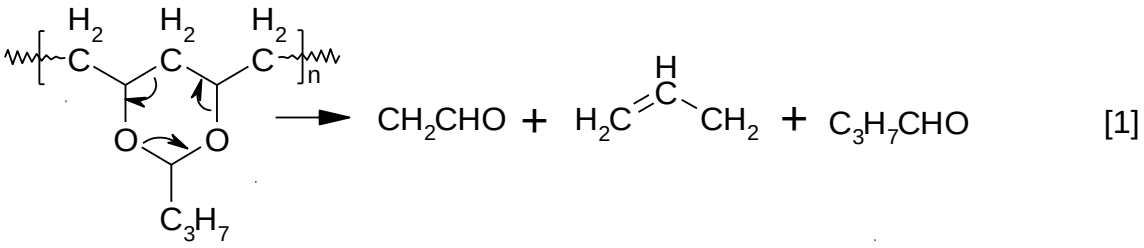

[1]

The relative quantities of butanal detected by MS are much less than those of species CH_2CHO (m/z 41) or H_2CCHCH_2 (m/z 43) [32]. It suggests that the above mechanism could not be the primary pathway for the butanal formation in the presence of Pd. A probable pathway for PVB could have involved Pd catalyst-enhanced formation of unsaturated hydrocarbon bonds from the ketone group as shown below:

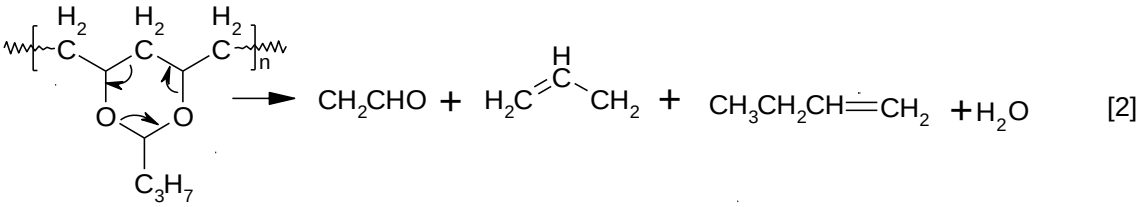

[2]

Hence, several techniques (UV-vis, TEM, GC-MS) can be used to follow the thermally induced changes in the polymer matrix in the presence of metal ions. PVB is a co(polymer) containing hydroxyl, acetate, vinyl, carbonyl and cyclic acetyl functional groups on which metal nanoparticles can be anchored. Figure 1 illustrates the procedure for the preparation of supported catalyst using the present approach.

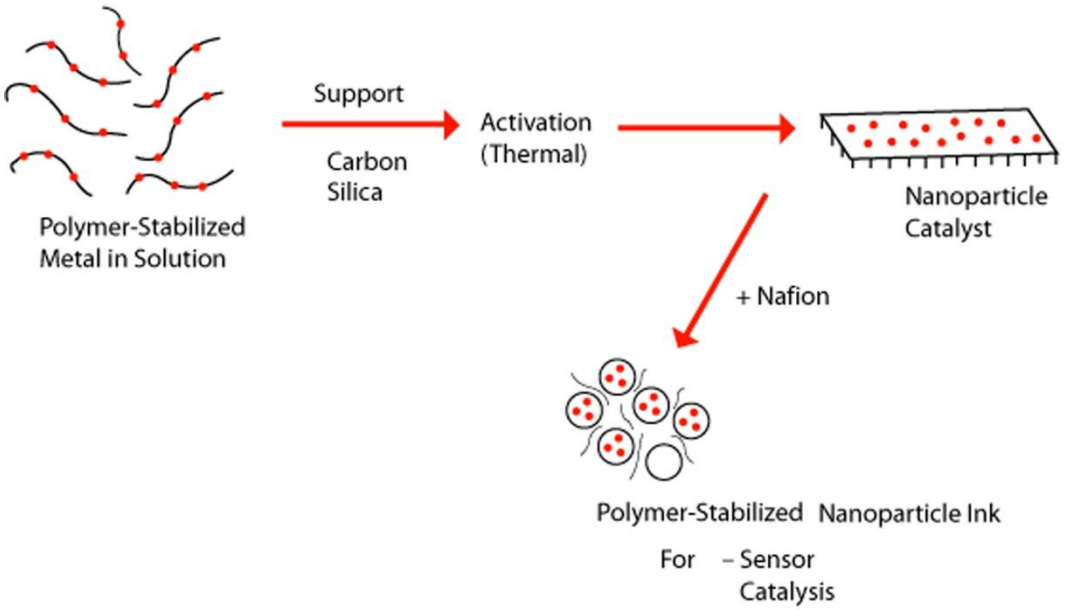

Figure 1. Schematic illustration of the procedure for the synthesis of polymer-stabilized nanoparticles

Thin films of PVB and PVB-metal nanoparticles (PVB-Pd ~ 2.13 μg Pd/g solid film) coated on glass slides were thermally treated for 5 hours at different temperatures and optical microscope with a digital camera was used to observe the morphology of the resulting film at room temperature. Unlike the non-metal containing PVB samples (Fig. 2A), the OM images of the PVB-Pd samples show some pattern of organization on the surface – some darker areas lie in between light colored areas (Fig. 2B). The darkened areas of the heated metal-polymer films are probably due to the self-organization of the metal-containing complexes and the degradation of the polymers while the brighter background fields represent the PVB matrix.

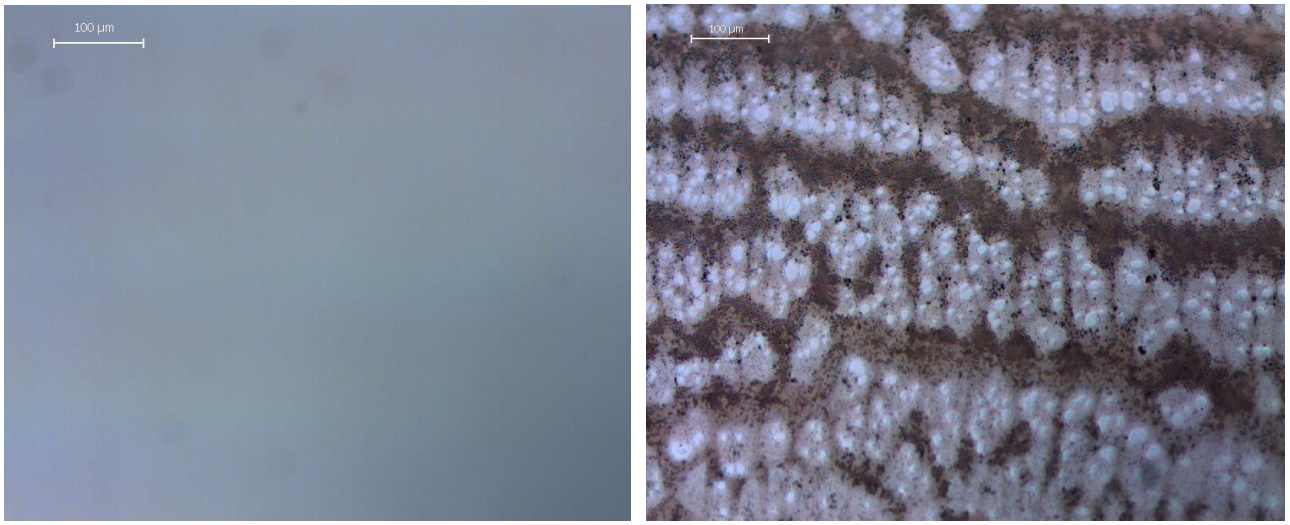

A **B**

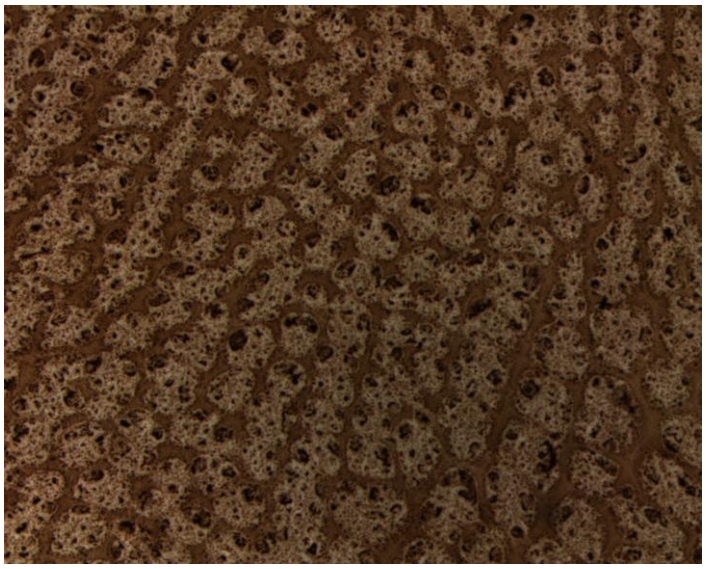

C

Figure 2. A. OM image of PVB film thermally activated at 200^{o}C for 5 hr; B. OM image of PVB-Pd film thermally activated at 200^{o}C for 5 hr; C. OM image of PVB-Pd composite film thermally treated at 200^{o}C for 48 hours

We attribute the characteristic features observed in the metal containing samples as resulting from the interaction of the metal ions with the functional groups in the polymer backbone. The presence of Pd catalyzes the PVB degradation with subsequent metal ion reduction for nanoparticle formation. Unlike the metal containing samples, the OM image color of the PVB only sample did not change from its room temperature appearance (not shown) even at 200^{o}C (Fig. 2A). The lack of color change is in agreement with the result obtained by Liu et al. [33] when purified PVB was heated at 120^{o}C for 2 hours. The PVB-Pd sample heated at 200 ^{o}C was further subjected to extended thermal treatment time at 200 ^{o}C for 48 hours and the result shown in Fig. 2C confirms possible formation of nanoparticles and the degradation of the polymers. The degradation of the polymer is evident in the figure. The patterns and features of the annealed surface may be unique to each type of metal-polymer interaction. These results show evidence of structural changes in the polymer film and possible formation of metal nanoparticles. To further confirm the variation of the structure of PVB and the formation of metal nanoparticles, the optical absorption and transmission spectra (UV-vis spectral) of PVB-metal composite and TEM analysis were undertaken.

Fig. 3 exhibits the absorption spectra of PVB and PVB-Pd films exposed to various temperatures for 5 hours. The UV-vis spectral analysis shows that at room temperature (Fig. 3A), the PVB only sample (without Pd) spectra exhibits absorption band at around UV-vis spectral profile with an absorption maximum at 415 nm and a small shoulder at 390 nm. The absorption band observed for PVB only is expected for hydroxyl containing groups. It reflects a probable $n \rightarrow \pi^{*}$ electronic transition characteristic of oxygen lone pair electrons due to the OH groups, the acetyl C═O and C─O─C cyclic groups present in the polymer backbone. These functional groups are typically involved in intramolecular and intermolecular hydrogen bonding. With the addition of Pd metal ions, a shift in the

maximum absorption peak is observed to result to a maximum absorption peak at 432 nm for the Pd containing films. Further, other peaks and shoulders are observed including peaks at 384 nm and 472 nm. The presence of metal ions lowers the magnitude of the absorption peak and gives rise to the appearance of other absorption peaks. The Uv-vis results obtained in the presence of Pd in the polymer contrasts with the result observed and attributed to n $\rightarrow\pi^*$ electronic transition found in PVB only sample but shows that the presence of Pd induces a shift in the absorption peaks [33].

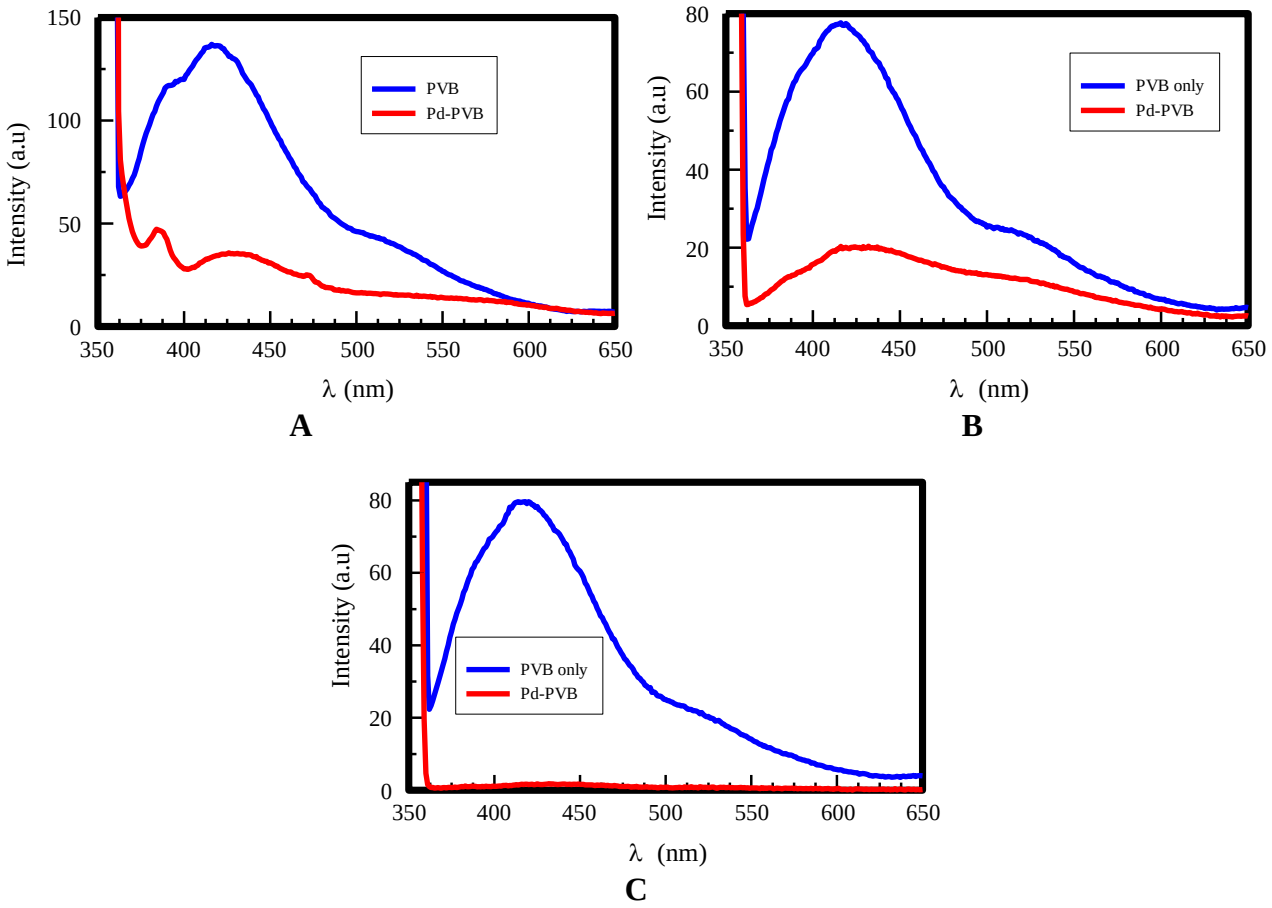

Figure 3. A. UV-vis absorption spectra for films held at room temperature for 2 hr; B. UV-vis absorption spectra for film samples treated at 100^{o}C for 2 hr; C. UV-vis absorption spectra for film samples activated at 200^{o}C for 2 hr

As the heating temperature is increased (Fig. 3b – 3c), the intensity of the maximum absorption peak band at the 415 - 432 nm range decreases for all samples but the UV-vis spectrum broadens only for the metal containing samples. Pd (also Pt) absorption in all ranges of UV-vis spectrum is known to occur and this gives evidence to support the formation of metal nanoparticles as the temperature is increased (fig. 3b – 3c) [34]. The changes in absorption band indicate that the size of the metal nanoparticles formed altered with temperature – a factor in the reduction process.

Relative to its room temperature behavior, the Pd-PVB nanocomposite has its maximum absorption peak shifted to 427 nm when the sample was heated to 100^{o}C. As the sample heating

temperature was raised to 200^{o}C, the absorption band peak observed within the 380 – 390 nm range at the lower temperatures was totally eliminated (Fig. 3c). As Fig. 3c shows, the Pd-PVB film shows absorption in all UV-vis ranges after thermal treatment at 200^{o}C. Our interpretation is that heating PVB alone to 200^{o}C in absence of Pd metal leads to some minor polymer chain degradation, thereby reducing the available oxygen lone pair electrons in the chain that is reflected in the UV-vis absorption characteristic of n $\rightarrow\pi^{*}$ electronic transition. In the presence of Pd, the thermal degradation of PVB is enhanced with the formation of metal nanoparticles. The decrease and broadening of UV-vis reflect these two processes. The inference from the results is the suggestion that the metal ions added in the polymer enhance the thermal degradation of the polymer matrix with subsequent reduction of the metal ions to their zero valent state. It seems that the formation of metal nanoparticles starts slowly at room temperature but it accelerates with rise in temperature. The result also suggests that within the temperature range of our study, the Pd catalyzed PVB-degradation is highly favored as the temperature is raised above 100^{o}C – an evidence of the importance of temperature in the PVB-metal nanoparticle stabilization process.

While the results in Fig. 3 demonstrate the significance of temperature in the PVB-metal interaction, a further examination of the effect of time on the thermal treatment of the

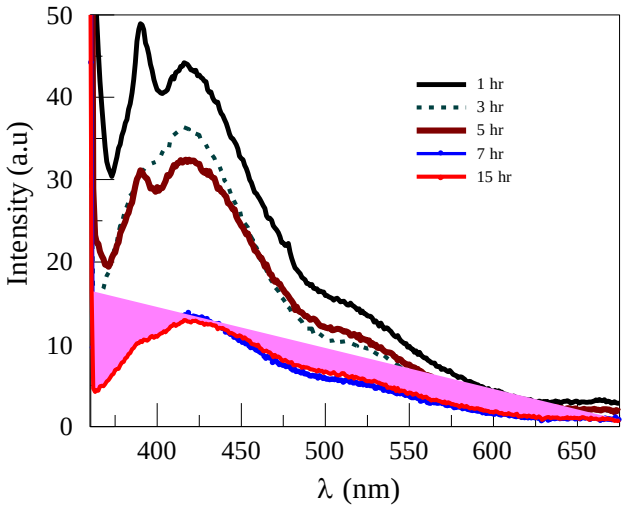

Figure 4. UV-vis absorption spectra for PVB-Pd composite film treated at 200^{o}C for different time lengths

PVB-Pd composite at 200^{o}C is shown in Fig. 4. As the thermal treatment time increased, changes in the polymer-metal complex is made manifest by observed changes with the absorption bands in both ultra violet (UV) as well as visible (vis) regions. The band at 390 nm decreased as well as the band with maximum peak at 415 nm. The broadening of the peaks with nanometal particles formation is also apparent. After 7 hours at 200^{o}C, it appears there is a complete reduction of palladium to zero-valent nanoparticles since further extension of the activation time to 15 hours did not result to any significant changes in the absorption band intensity.

The formation and growth of metal nanoparticles was examined with TEM. Fig. 5 shows the TEM images of Pd nanoparticles stabilized in PVB. The figure shows uniformly distributed cluster of metal nanoparticles around a corona region (Fig. 5B) i.e. metal nanoparticles cluster forming a shell that surrounds a polymer core. Inside the corona, few particles (if any) with average particle size much less than those outside the corona are found. Around the edge of the corona, the nanoparticles are seen clustered. Spherical particles of nm size ranges are seen. Evidence of self-assembly is apparent in fig. 5 and is a function of the polymer matrix functionality. Typically, a multi-block copolymer will chemically interact selectively with reactive metal complexes due to the differing solubility and coordination properties of the blocks. For PVB, possible interactions with Pd ions can occur with the several OH group on the polymer or the C=O of the acetate group or the 1,3-dioxane ring. The figure gives credence to the possible use of the method to decorate a substrate for specific applications.

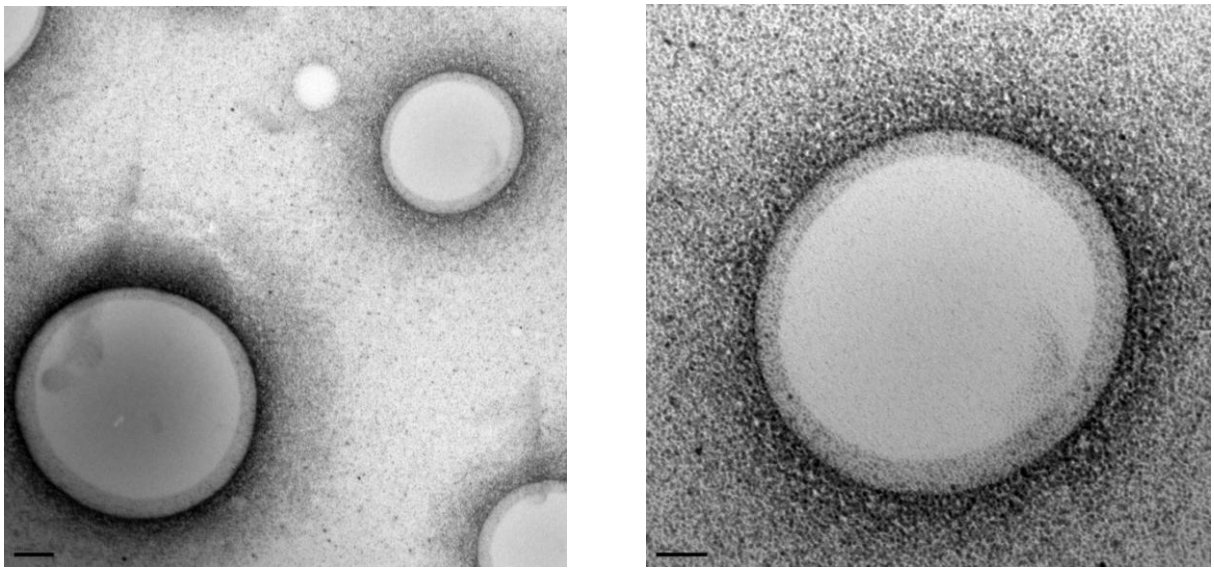

Scale Bar = 100 nm
A

Scale Bar = 50 nm
B

Figure 5. A. TEM image of PVB-Pd film treated at 200^{o}C for 2 hours (Scale Bar = 100 nm); B. A magnification of TEM result from fig. 5A showing a corona and nanoparticle core-shell for PVB-stabilized Pd nanoparticles (Scale Bar = 50 nm)

Fig. 6 shows XRD patterns obtained for PVB-palladium ink used to catalyze or decorate carbon nanotubes (CNT) (Pd/CNT). The XRD patterns for Pd/CNT show diffraction peaks at 2θ equal to 40.49^{o}, 46.97^{o}, 68.39^{o}, 82.31^{o} and 86.83^{o}, respectively corresponding to the (111), (200), (220), (311), and (222) planes of Pd face-centered cubic (fcc) crystal structure. The average particle size was estimated from the Scherrer equation [35], $\beta = \kappa\lambda / D\cos\theta$, where κ is the shape factor (0.9), λ is the X-ray wavelength, D is the full width at half maximum (FWHM) of the diffraction peak. The metallic Pd (222) reflection at 250^{o}C was used to estimate the size of the nanoparticles and found to be in the range 3.5 - 10 nm.

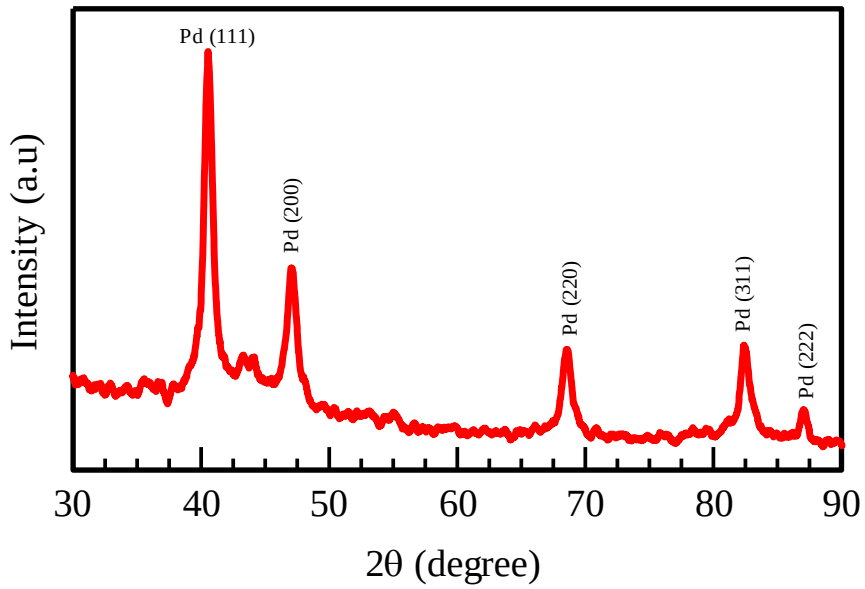

Figure 6. XRD patterns of polymer-stabilized metal nanoparticles activated at 275°C on CNT support

3.1 Electrochemical Characterization

Cyclic voltammetric exam was used to evaluate the electrocatalytic activity of the polymer-stabilized Pd zero-valent nanoparticles generated by the current method. Here, the reversible electrochemical reaction involving the reduction of ferricyanide to ferrocyanide (see equation 3) is used to evaluate the possible generation of zero-valent metal nanoparticles:

$$Fe(CN)_6^{3-} + e^- \leftrightarrow Fe(CN)_6^{4-} \qquad [3]$$

Because an electron exchange occurs as ferricyanide is transformed into ferrocyanide, the reaction can be used to characterize the electrode surface area (proportional to the number of metal nanoparticles) of the working electrode using Randles-Sevcik [36] equation. The equation relates the concentration and the transient's peak current, i_p, as follows:,

$$i_p = 0.4463nFAC(nFvD/RT)^{1/2} \qquad [4]$$

where i_p is the current, n = number of electrons, A = area of electrode, D = diffusion coefficient, T = temperature (K), F = Faradays constant, and R = gas constant.

The reversible ferricyanide system was used to characterize the electrocatalytic activity of the Pd-nanoparticle. Fig. 7 compares the electrocatalytic activity of uncatalyzed graphite and PVB-stabilized Pd catalyzed nanoparticles in 0.1 mM ferricyanide. The figure shows that the catalyzation method improved the electrocatalytic activity of the carbon substrate. The metal nanoparticle catalyzation increases the active electrode surface area by an order of magnitude (Pd increases the active area by about 214% compared to the uncatalyzed carbon)

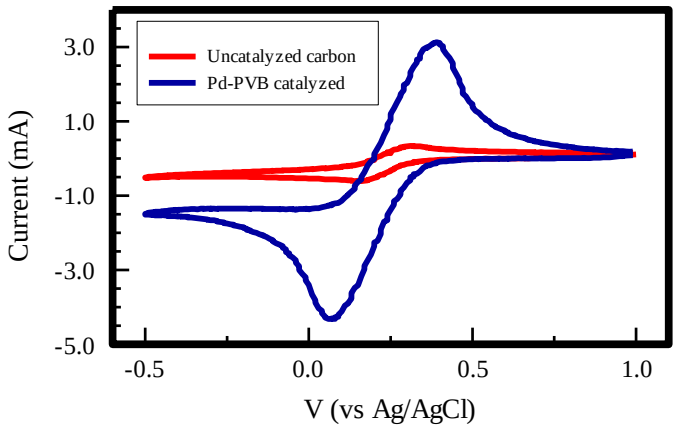

Figure 7. CV of Pd-catalyzed (with PVB stabilized nanoparticles) and uncatalyzed surfaces in 0.1 mM Ferricyanide (scan rate: 50 mV/s)

3.2 Electrocatalysis using Pd-Stabilized Nanoparticles

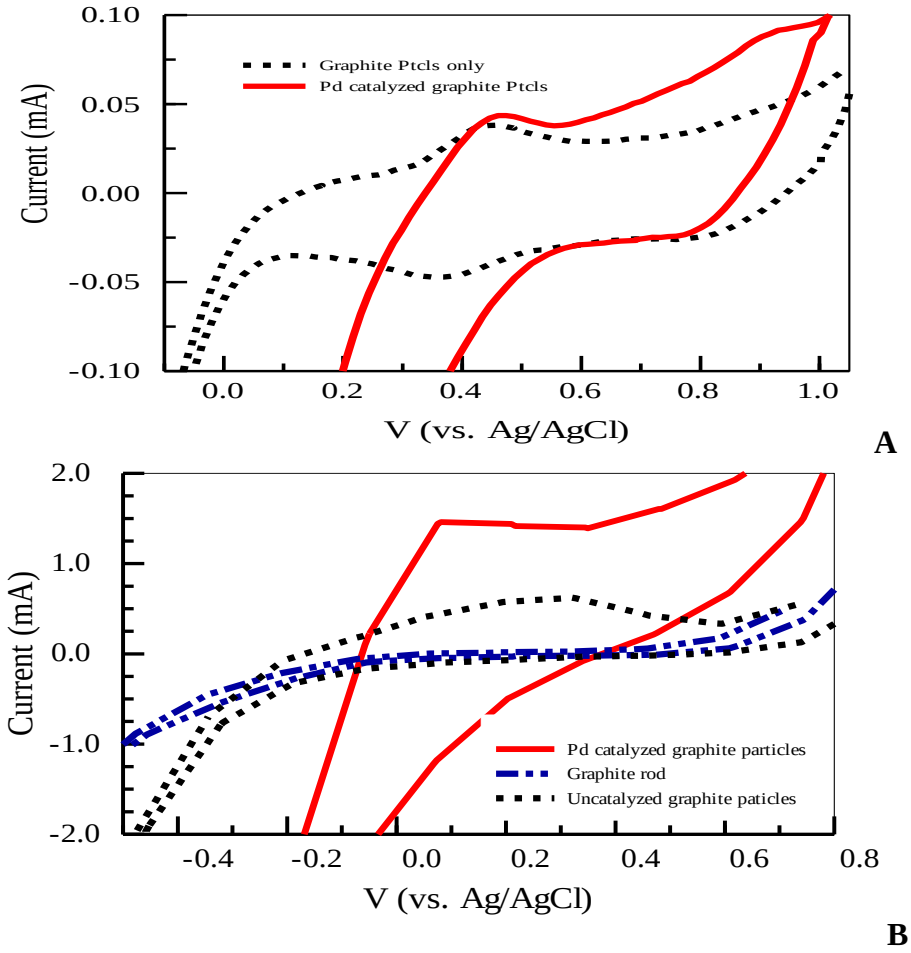

Figure 8. A. CV of uncatalyzed and Pd-catalyzed (with PVB-stabilized nanoparticles) graphite particles in oxygen saturated 0.5 M H_2SO_4 (Scan rate: 20 mV/s); B. Electrocatalysis effect: Pd nanoparticles on the oxidation of 8 mM H_2O_2 in 0.1 M phosphate buffer solution (pH 7). (Scan rate: 50 mV/s)

Although the synthesis approach described above is general for any heterogeneous metal nanoparticle catalysts, some specific reactions in electrocatalysis are used here for the illustration of the approach. In direct methanol fuel cell, oxygen reduction with Pt-based catalysts is easily depolarized. Hence, the use of Pd nanoparticles as methanol-tolerant catalyst is a subject of current interest. Graphite particles made more active (catalyzed) with Pd using our approach was evaluated for oxygen reduction. Figure 8A illustrates CV for uncatalyzed and Pd-catalyzed graphite particles in 0.5 M H_2SO_4 under oxygen atmosphere. As can be seen in the figure, the presence of Pd enhances the oxygen reduction current – evidence of improved electrocatalytic activity. It should be noted here that the Pd loading is exceedingly very low (~ 1.84 μg/g graphite particles or 0.184 wt% Pd) compared to the currently used amount in fuel cells (20 wt % Pd). Considering the small amount of metal loading used and the improved catalytic performance observed, the approach has some promise and merit. The performance of polymer-supported Pd nanoparticle as methanol-tolerant oxygen electrocatalyst is described in our forth coming publication.

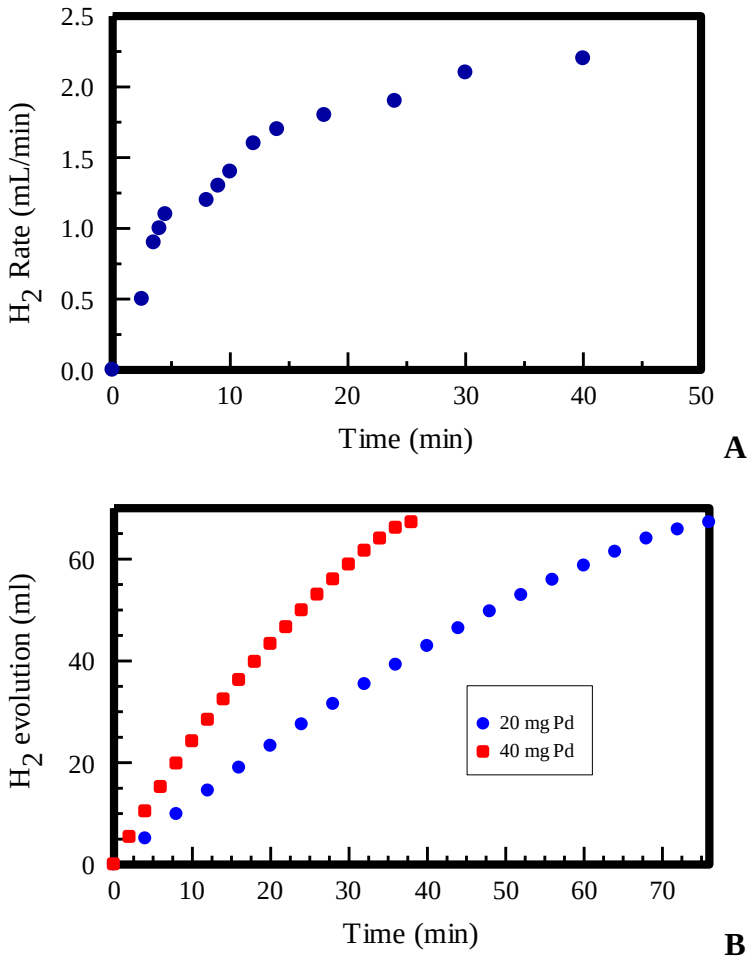

Figure 9. A. Hydrogen generation from electroless Ni catalyzed sodium hypophosphite hydrolysis (2 min-deposited electroless Ni using PVB-stabilized Pd nanoparticles as seed catalyst for electroless nickel deposition); B. Hydrogen generation from the hydrolysis of ammonia borane using PVB-stabilized Pd nanoparticles deposited on TiO_2 as catalyst

The detection of hydrogen peroxide generated from enzyme (glucose oxidase) catalyzed oxidation of glucose forms the basis of glucose biosensor. An effective method for the construction of a biosensor involves the immobilization of the enzyme on metal nanoparticles. Thus, electrocatalysis of hydrogen peroxide by the metal nanoparticles used for enzyme immobilization is a prerequisite for the choice of metal type. Polymer-stabilized Pd nanoparticles prepared with PVB as described in this work was tested for the oxidation of hydrogen peroxide in a phosphate buffer solution. The electrocatalysis of hydrogen peroxide is compared for graphite rod, Pd-catalyzed and uncatalyzed graphite particles in Fig. 8B. The figure shows that hydrogen peroxide electrocatalysis on PVB-stabilized nanoparticles is more active than in the absence of the metal nanoparticles. Based on this finding, we developed glucose biosensor based on the use of polymer-stabilized metal nanoparticles [37]. In addition to the two illustrative examples given above in electrocatalysis, the catalysts prepared by this approach were used for the catalysis of hydrolysis reactions for hydrogen generation. In Figure 9A, Pd nanoparticles produced by the described method was first used to prepare electroless Ni catalyst that was subsequently used for hydrogen generation from SBH while in Fig 9B, the palladium nanoparticles deposited on TiO_2 were directly used for the hydrolysis of AB for hydrogen generation:

$$NaBH_4 + 2H_2O \xrightarrow{Ni\ catalyst} NaBO_2 + 4H_2 \qquad [5]$$

$$NH_3BH_3 + 2H_2O \xrightarrow{Pd\ catalyst} NH_4BO_2 + 3H_2 \qquad [6]$$

In the results, the catalytic ability of the deposited polymer-stabilized nanoparticles are demonstrated. The amount of Pd loading required to initiate electroless Ni plating is comparatively low relative to the Pd loading required for direct catalysis of either SBH or AB hydrolysis. Thus, the choice of the two-step approach – polymer-stabilized Pd nanoparticles followed by electroless plating – is informed by the cost of Pd relative to nickel. These results are but some evidence of the wide applicability of the approach for catalyst preparation.

4. CONCLUSION

The results show that the approach described in this work is most applicable for polymers that contain transition metal-ligand forming functional groups such as hydroxyl, ketone, carboxylic acid, vinyl groups, etc. The method can be used to generate small sized and well dispersed catalytically active metal nanoparticles (stabilized by a polymer matrix) as heterogeneous catalysts on most supports including the preparation of electrocatalysts for fuel cells. PVB-stabilized Pd nanoparticles were successfully prepared by thermolysis at relatively low temperature without the use of chemical reducing agent such sodium borohydride. The generated nanoparticles were characterized by UV, TEM, XRD, OM and electrochemical techniques. Evidence of formation of PVB-stabilized zero-valent metal nanoparticles was elucidated through the use of TEM, XRD and electrochemical techniques. The use of the approach for the synthesis of heterogeneous catalysts including electrocatalysts is suggested

and was illustrated with examples from catalysis of chemical hydrolysis and oxidative and reductive electrocatalysis.

ACKNOWLEDGMENTS
We acknowledge the support of the Partnership for Research and Education in Materials initiative of the National Science Foundation under NSF Award 0351770, NSF Grant No. DMR-0351770.

References

1. C. Roth, A. J. Papworth, I. Hussain, R. J. Nichols and D. J. Schiffrin, *J. Electroanal. Chem.*, 581 (2005) 79
2. M. P. Mallin and C. J. Murphy, Nano Lett. 2 (2002) 1235
3. T. Trindade, P. O'Brien, N. L. Pickett, *Chem. Mater.* 13 (2001) 3843
4. B. Coq, J. M. Planeix, V. Brotons, *Appl. Catal.* A 173 (1998) 175
5. R. Shenhar, T. B. Norsten, V. M. Rotello, *Adv. Mater.* 17 (2005) 657
6. R. W. J. Scott, O. M. Wilson and R. M. Crooks, *Chem. Mater.* 16 (2004) 5682
7. J. –J. Li, X. –Y. Xu, Z. Jiang, Z. –P. Hao and C. Hu, *Environ. Sci. Technol.* 39 (2005) 1319
8. H. Lang, S. Maldonado, K. J. Stevenson and B. D. Chandler, *J. Am. Chem. Soc.* 126 (2004) 12949
9. R. W. J. Scott, C. Sivadinarayana, O. M. Wilson, Z. Yan, D. W. Goodman and R. M. Crooks, *J. Am. Chem. Soc.* 127 (2005) 1380
10. S. Mukerjee, S. Srinivasan and M. P. Soriaga, *J. Electrochem. Soc.* 142 (1995) 1409
11. A. Lekhal, B. J. Glasser, J. G. Khinast, *Chem. Eng. Sci.* 59 (2004) 1063
12. J. A. Bergwerff, T. Visser, B. R. G. Leliveld, B. D. Rossernaar, K. P. De Jong, B. M. Weckhuysen, *J. Am. Chem. Soc.* 126 (2004) 14548
13. M. K. Van der Lee, A. J. Van Dillen, J. H. Bitter and K. P. de Jong, *J. Am. Chem. Soc.* 127 (2005) 13573
14. M. Che, Z. X. Cheng, C. Louis, *J. Am. Chem. Soc.* 117 (1995) 2008
15. Lashdaf M, J. Lahtinen, M. Lindblad, T. Venalainen, A. O. I. Krause, *Appl. Catal.* A-General, 276 (2004) 129
16. J. J. Wu, C. H. Tseng *Appl. Catal. B- Environmental*. 66 (2006) 51
17. N. Toshima and T. Yonezawa, *New J. Chem.* 22 (1998) 1179
18. M. O. Nutt, J. B. Hughes and M. S. Wong, *Environ. Sci. Technol.* 39 (2005) 1346
19. R. Giordano, P. Serp, P. Kalck, Y. Kihn, J. Schreiber, C. Marhic and J. –L. Duvail, *Eur. J. Inorg. Chem.* 4 (2003) 610
20. W. Yu, M. Liu, H. Liu and J. Zheng, *J. Colloid & Int. Sc.* 210 (1999) 218
21. S. –H. Choi, S. Lee, S. –J. Kim, S. –H. Sohn, H. –D. Kang, Y. –P. Zhang, K. –P. Lee and J. –H. Chun, *Catal. Lett.* 105 (2005) 59
22. E. Ramirez, S. Jansat, K. Philippot, P. Lecante, M. Gomez, A. M. Masdeu-Bulto and B. Chaudret, *J. Organometallic Chem.* 689 (2004) 4601
23. R. W. J. Scott, O. M. Wilson, S. –K. Oh, E. A. Kenik and R. M. Crooks, *J. Am. Chem. Soc.* 126 (2004) 15583
24. S. Yang, Y. Wang, Q. Wang, R. Zhang and B. Ding, *Colloids and Surfaces* 301 (2007) 174
25. S. -H. Choi, S. Lee, S. -J. Kim, S. -H. Sohn, H. -D. Kang, Y. -P. Zhang, K. -P. Lee, J. -H. Chun, *Catalysis Letters* 105 (2005) 59
26. Y. Shin, I. -T. Bae, B. W. Arey and G. J. Exarhos, *Mater. Lett.*, 61 (2007) 3215
27. E. E. Kalu, *Plating & Surf. Finishing* 85 (1998) 74
28. A. S. Kuruganti, K. S. Chen, and E. E. Kalu, Electrochemical & Solid State Lett., 2 , (1999) 27
29. E. E. Kalu, *Plating & Surf. Finishing*, 87 (2000) 62

30. M. Rakap, E. E. Kalu, S. Özkar, *Int. J. Hydrogen Energy* 36 (2011) 1448
31. M. F. Bakht, *Pakistan J. Sci. Ind. Res.*, 26 (1) (1983) 35
32. E. E. Kalu, unpublished data (2000)
33. R. Liu, B. He and X. Chen, *Polymer Degradation and Stability*, 93 (2008) 846
34. X. Sun, Y. Du, L. Zhang, S. Dong, E. Wang, *Anal. Chem.*, 78 (2006) 6674
35. A. L. Patterson, *Physical Review* 56, (1939) 978
36. J. E. B. Randles, *Trans. Faraday Soc.* 48 (1952) 828
37. D. Foxx and E. E. Kalu, *Electrochem. Commun.*, 9 (2007) 584